



## Regionally and seasonally differentiated primary production in the North Atlantic

SHUBHA SATHYENDRANATH,<sup>\*,†</sup> ALAN LONGHURST,<sup>†</sup>  
CARLA M. CAVERHILL<sup>†</sup> and TREVOR PLATT<sup>†</sup>

(Received 8 August 1994; in revised form 27 March 1995; accepted 30 March 1995)

**Abstract**—A bio-geochemical classification of the N. Atlantic Basin is presented according to which the basin is first divided into four primary algal domains: Polar, West-Wind, Trades and Coastal. These are in turn sub-divided into smaller provinces. The classification is based on differences in the physical environment which are likely to influence regional algal dynamics. The seasonally-differentiated parameters of the photosynthesis–light curve ( $P$ – $I$  curve) and parameters that define the vertical structure in chlorophyll profile are then established for each province, based on an analysis of an archive of over 6000 chlorophyll profiles, and over 1800  $P$ – $I$  curves. These are then combined with satellite-derived chlorophyll data for the N. Atlantic, and information on cloud cover, to compute primary production at the annual scale, using a model that computes spectral transmission of light underwater, and spectral, photosynthetic response of phytoplankton to available light. The results are compared with earlier, satellite-derived, estimates of basin-scale primary production.

### INTRODUCTION

There are two components to the problem of using satellite, sea-surface chlorophyll fields to compute basin-scale or global primary production: (i) the choice of an appropriate local model and (ii) its extrapolation to the large scale. In this paper we explore the extrapolation of an established local model over a rational, ecological geography of the North Atlantic Ocean.

Several procedures are available to estimate local marine primary production in the ocean, using light-dependent models of photosynthesis. They require the following information: the sub-surface light field just below the sea surface ( $I_0$ ) as a function of the time ( $t$ ); the distribution of diffuse attenuation coefficient for downwelling light ( $K$ ) and the chlorophyll ( $B$ ) with depth ( $z$ ) in the water column; and finally, as functions of depth, the parameters of the photosynthesis–light ( $P$ – $I$ ) curve: its initial slope ( $\alpha^B$ ) and the assimilation number ( $P_m^B$ ), both normalized to  $B$  (Sathyendranath and Platt, 1993).

Given this information, we can compute the light available at depth  $z$  and time  $t$ , and use this to compute the instantaneous photosynthetic rate at that depth, which can then be integrated over time and depth to obtain daily, water-column primary production.

It follows that any computation of primary production at large scales would also require

---

<sup>\*</sup>Oceanography Department, Dalhousie University, Halifax, Nova Scotia, Canada B3H 4J1.

<sup>†</sup>Biological Oceanography Division, Bedford Institute of Oceanography, Dartmouth, Nova Scotia, Canada B2Y 4A2.

such information, but resolved appropriately in space and time. Satellites provide some, but not all, of the required information with appropriate spatial and temporal resolutions: thus, cloud fields can be combined with atmospheric transmission models to obtain  $I_0$  (Bishop and Rossow, 1991); sea-surface colour fields contain information on near-surface chlorophyll  $B$ , and since  $B$  and  $K$  are closely related, at least in open-ocean waters, we can also infer something about  $K$  (Gordon and Morel, 1983; Sathyendranath and Morel, 1983). But satellite remote-sensing provides neither depth-resolved  $B$  or  $K$ , nor the  $P-I$  parameters (but see Topliss and Platt, 1986).

Therefore, large-scale computations of primary production must be approached by combining satellite and *in situ* observations, and this will require techniques for extrapolating *in situ* observations in space and time, to match the satellite data base. The relevant properties to be extrapolated are the parameters that define the shape of the chlorophyll profile (and therefore of the attenuation coefficient  $K$ ), and the  $P-I$  parameters. Although some progress has been made in recent years in the areas of remote sensing and modelling primary production, the problem of extrapolation of local measurements to large scales has remained unresolved.

Two principal methods of achieving the required extrapolation are available to oceanographers: They may assume either that the oceans can be treated as a biological continuum, or that spatial discontinuities between ecological entities should be recognized.

Facing the same problem of extrapolating local parameters to the global scale, terrestrial ecologists have no such choice, for the ecological differences between forest, savanna and grasslands are so profound as to be reflected in most human languages. Terrestrial ecosystem models to compute global production (e.g. Melillo *et al.*, 1993) are usually partitioned among twenty or more vegetation types, mapped on the land surface from satellite images: different parameter values are appropriate in modelling growth of each vegetation type, though all are linked by common assumptions concerning the biochemistry of photosynthesis, and the physiological response of plants to rainfall, sunlight, temperature and nutrients. A few regional characteristics (ambient rainfall, temperature and soil type) may be sufficient to specify zones occupied by different terrestrial vegetation biomes.

Conversely, despite the high degree of variability that has long been known to exist in both physiological and ecological rates in the marine ecosystem, computations of global production in the ocean are rarely partitioned as thoughtfully as are the comparable computations for the land biota. Usually, broad latitudinal zones, or complete ocean basins, have been thought to suffice as compartments for the computation of global primary production in the ocean. Ecological continuity is generally assumed when one-dimensional models of biological processes in the ocean are incorporated into general circulation models or other global simulations (e.g. Toggweiler, 1990), or if ecological compartments are invoked, then these often represent no more than a distinction between coastal and oceanic environments. The assumption of ecological continuity requires either that the parameters of the biological model remain constant everywhere or that they always respond in the same way to changes in the environment. But biological responses, which are often species-dependent, are complicated by species-succession and by the physiological state of the phytoplankton population (Platt *et al.*, 1992 and Platt *et al.*, 1993), so the potential for non-linearity in biological responses should not be overlooked.

In addition to variability in the  $P-I$  parameters, a principal difficulty in estimating

oceanic productivity from surface measurements arises from the regional differences in the vertical distribution of chlorophyll, an analogue of the structural diversity of terrestrial ecosystems. Morel and Berthon (1989) suggested that this problem might be avoided by presuming that surface chlorophyll values predict not only the total chlorophyll concentration in the euphotic zone (as established for example by Lorenzen, 1970; Smith, 1981; Platt and Herman, 1983), but also chlorophyll distribution as a function of depth. But are the relationships between surface chlorophyll and vertical distribution consistent enough for our purpose?

We find that such relationships are sufficiently variable that we are led to adopt an approach in which the computation of primary production is partitioned to reflect the realities of the regional diversity of ocean ecology. The concept of a dynamic biogeography of the oceans, comprising unique biogeochemical provinces having seasonally-predictable algal growth dynamics, was advanced by Platt and Sathyendranath (1988). The use of local algorithms to compute basin-scale production partitioned in this way was then illustrated by Platt *et al.* (1991), based on a simple set of geographical compartments for the North Atlantic: three depth zones (shelf, slope, deep) and four latitude zones (Subarctic, Temperate/Transitional, Subtropical, Equatorial).

In this paper we take the next logical steps.

- (i) We propose a method for partitioning the biogeochemical complexity of the North Atlantic, using criteria that are sensitive to regional differences in algal ecology, and to discontinuities in the near-surface circulation.
- (ii) Then, using a comprehensive archive of North Atlantic chlorophyll profiles, we test and refine the boundaries between the proposed domains and provinces.
- (iii) Next, we test whether basin-scale relationships can be established between chlorophyll concentration at the surface and its vertical distribution, such that a partition into provinces would be superfluous.
- (iv) Finally, we use the local algorithm of Platt and Sathyendranath (1988), slightly modified with respect to the light transmission part, to compute basin-scale primary production for the North Atlantic (north of 10°S and west of 1°E), to illustrate the value of using a comprehensive data archive to parametrize the chlorophyll profile and to investigate the utility of a finer and more rational partitioning of the North Atlantic basin into biogeochemical provinces.

## A DYNAMIC, BIOGEOGRAPHIC CLASSIFICATION OF THE NORTH ATLANTIC BASIN

The arguments on which we base our proposed biogeographical classification for the N. Atlantic require some explanation:

(1) The possible scales of extrapolation and interpolation are obviously limited by the available data and their regional and seasonal coverage. Though sufficient data are now available to generate monthly-averaged climatological atlases of some physical and chemical oceanographic variables, with a grid resolution of one or two degrees, there are so few observations of the biological parameters required in this study that binning and averaging procedures have to be carried out over much coarser spatial and temporal scales.

(2) We are constrained, therefore, to use regional oceanography to define compartments within which we expect seasonal uniformity of the major processes that govern

biological processes: these will be our biogeographic provinces. If numerous, well-distributed data were available, natural boundaries between regions might be apparent in the data fields themselves. But we did not expect, and did not find, that the available data were sufficient for this. Thus, other sources of information have to be used to identify the boundaries of the provinces: as well as the location of divergences, convergences and other circulation features, we examined the effects of turbulent diffusion, thermal stabilization and geostrophic adjustment, all of which have significant regional consequences for nutrient forcing and algal growth dynamics.

(3) Because of the spatial and temporal variability of seasonal biological events, any partitioning of the ocean into provinces must be based on dynamic boundaries that respond to changes in oceanographic forcing. For practical reasons, it is desirable that the boundaries should correspond to features observable by remote sensing, such as discontinuities of the slope and elevation of the sea surface, or of the sea-surface chlorophyll and thermal fields.

(4) The concept of a biological continuum should be applicable within each province and season, so that the *in situ* properties that are parametrized should be either stable or predictable. It is paramount that any biogeochemical partitioning of the ocean be sensitive to the principal fields that force algal dynamics: local wind stress, local solar radiation, and distantly-forced geostrophic adjustment of mixed-layer depths.

(5) The total number of provinces should not be so large that the problem of locating representative oceanographic data becomes intractable, especially since climate-change studies should include information on both inter-annual and intra-annual variability. Thus, from purely practical considerations, we suppose that more than about 50 provinces globally would be unreasonable.

(6) As we shall discuss, the available observations of  $P-I$  and chlorophyll profiles are insufficient to describe mean seasonal conditions within even this number of provinces. So criteria have to be developed for extrapolating results from one region to another. To do this, we rely on locating analogous regions where environmental conditions parallel those in regions for which we have adequate  $P-I$  and chlorophyll profile data. Extrapolations can be made between provinces with similar oceanographic conditions, but not necessarily between adjacent provinces.

(7) The resolution and the precision required of the input parameter fields is dictated by the sensitivity of the computed field (e.g., primary production) to errors in the input fields. The errors introduced in the computed field due to errors in the input parameter fields must lie within an acceptable range. If small uncertainties in an input field propagated to large errors in the computed field, then we would conclude that the computational procedure was inherently unstable, and that no useful conclusions could be drawn from it. But if the computations are insensitive to variations in the parameter field, it is adequate to treat the parameters, for the purpose of the computation, as constants. The greater the sensitivity of the computed field to the input field, the greater would be the need for higher resolution in the input field. However, random errors would be more tolerable than systematic errors, if it were planned to average the results over many pixels.

With these considerations in mind, we can describe how we partition the N. Atlantic into the suite of biogeochemical provinces illustrated in Fig. 1. In our description of the regional oceanography we have tried to follow Tomczak and Godfrey (1994).

Classical, one-dimensional models of the spring bloom (e.g. Sverdrup, 1953) require forcing only by local radiation and wind stress, but distant forcing of mixed-layer dynamics

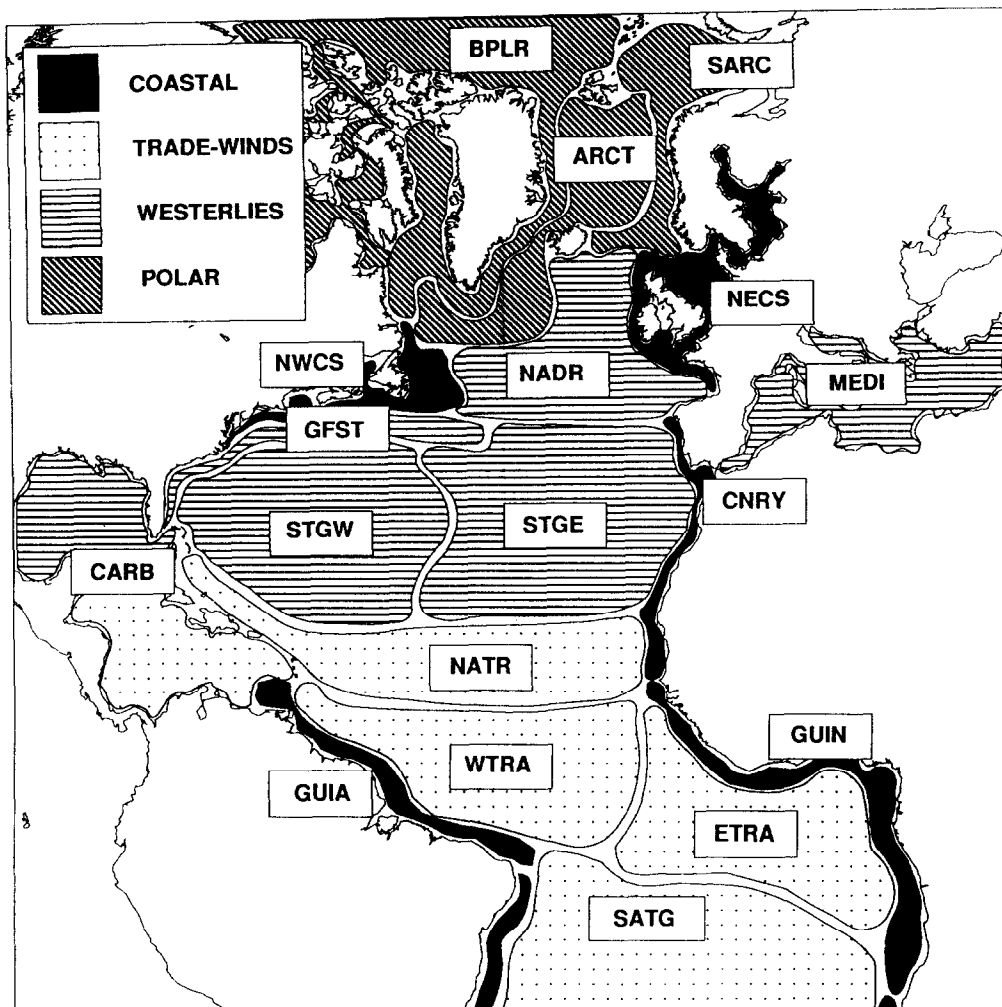


Fig. 1. Approximate areas occupied by the primary ecological domains and secondary provinces proposed for the Atlantic Ocean in this study. In addition to the North Atlantic provinces described in the text, this figure shows also the South Atlantic provinces: Benguela Current (BENG), Brazil Current (BRAZ), South Subtropical Convergence (SSTC), Falkland plateau (FLKD) and the northern part of the Subantarctic (SANT). Note that both the Caribbean and South Atlantic gyral provinces, as presently defined fall within the influence of both trades and westerly winds.

and hence phytoplankton growth is paramount over much of the ocean (Longhurst, 1993). Thus, regional differences in seasonal algal cycles, and other aspects of pelagic ecology, may reflect regional differences in mixed-layer dynamics, and so partitioning of the ocean must be compatible with regional, seasonal variations in these factors. Therefore, an analysis of the biological consequences of regional oceanography at all latitudes of the North Atlantic preceded both the drafting of a set of biogeochemical provinces, and an examination of a data archive of the  $P-I$  and chlorophyll-profile parameters.

We first identified four *primary biogeochemical domains*, each having unique physical characteristics likely to dominate their phytoplankton ecology. Each domain could be sub-

divided rationally into several *biogeochemical provinces*, each of about the dimensions likely to be useful as a component of a global system (Longhurst, 1995).

### *Polar Domain*

Three provinces constitute this high-latitude domain, and have in common the presence, especially in spring and early summer, of a brackish surface layer due to the melting of winter ice cover; this layer induces stability early in the season so that an algal bloom occurs as soon as surface irradiance is sufficient (Smith and Sakshaug, 1990), a process which may occur earlier than the induction of mid-latitude blooms by progressive vernal shoaling of the winter mixed layer:

*Boreal Polar (BPLR)*—Comprises the Arctic Ocean and its outflow through the Fram Straits and the Canadian Archipelago. These flows, and hence the province, are bounded by the East Greenland Polar Front and, less strongly, by the offshore boundaries of the West Greenland and the Labrador Currents. Characteristics of the domain are strongest in this province.

*Arctic (ARCT)*—Comprises the recirculation eddies of Atlantic water returning westwards from the Barents and Norwegian–Greenland Seas, bounded to the northwest by the East Greenland Polar Front and elsewhere by the Iceland Gap Front and the oceanic Polar Front across the North Atlantic and in the Nordic Seas (Johannessen, 1986).

*Subarctic (SARC)*—Comprises the flow of the warm North Atlantic Drift northwards into the Barents Sea bounded by the Norwegian Coastal Front and the Polar fronts of the Nordic and Barents seas.

### *West-Wind Domain*

This domain occupies the mid-latitude oceanic regions where westerly winds induce winter convective mixing, and spring blooms can be sufficiently described by Sverdrup's critical-depth model (Sverdrup, 1953) as a result of progressive shoaling of the deep winter mixed layer in response to increasing radiation and decreasing wind stress. Here, phytoplankton dynamics can be adequately described as a response to local forcing. We find it useful to recognize five provinces in this domain:

*Gulf Stream (GFST)*—Comprises the flow from Florida to the bifurcation in the Newfoundland Basin. We include the eddy fields along the immediate flanks of the current. Shorewards it is bounded by a strong thermal discontinuity at the surface, while seawards the 18°C surface isotherm is a useful limit.

*N. Atlantic Drift (NADR)*—Comprises the flow of the North Atlantic Current eastwards from Newfoundland, south of the Oceanic Polar Front to the Iceland–Faeroes Ridge, where it passes south of the Iceland Gap Front and into the Subarctic Province. East of the mid-Atlantic Ridge, meandering and eddying is enhanced.

*Subtropical Gyre (STGE and STGW)*—This is the poleward part of the North Atlantic anticyclonic gyre where it lies under the influence of the winter westerlies. The northern limb is the Azores Current originating in the Newfoundland Basin and the southern limit is the Subtropical Convergence. East and west, we place its boundaries seawards of the eddy fields of the boundary currents. We have subdivided the gyre into two provinces, east and west above the topography of the mid-Atlantic Ridge, recognizing ecological differences between the Sargasso Sea and the eastern basin.

*Mediterranean (MEDI)*—This marginal basin of the North Atlantic is considered to be a unique province for present purposes. Winter mixing is strong and localized because of complex coastal topography and orography.

#### *Trade-Wind Domain*

In the Trade-Wind Domain local wind mixing is constrained by high values of the Brunt-Väisälä frequency in the shallow pycnocline and high values of the Rossby internal radius of deformation, so that mixed-layer depth (and hence phytoplankton dynamics) may be determined principally by geostrophic adjustment to distant wind forcing (Light-hill, 1969; Emery *et al.*, 1984; Philander, 1985; Longhurst, 1993). We recognize five provinces within this domain:

*Tropical Gyre (NATR)*—Comprises the southern part of the anticyclonic gyre, south of the Subtropical Convergence, and of regions where winter mixing remains significant. Contains the westward flow of the North Equatorial Current around the southern limb of the anticyclonic gyre, so that the southern boundary is a seasonal convergence with the North Equatorial Countercurrent. Includes the offshore Guinea thermal dome and carries cold filaments from the Canary Current coastal upwelling.

*Western Tropical Atlantic (WTRA)*—Includes the seasonal flow of the North Equatorial Countercurrent and associated retroflexion eddies from the South American coast, and is characterized by seasonal Ekman suction (and algal blooms) along its northern boundary and seasonal thermocline deepening further south. The eastern boundary is the “hinge-line” at 20°W (Longhurst, 1993) about which seasonal tilting of the tropical thermocline occurs. Equatorial divergence occurs in the southeastern part of this province. The boundary to the southwest is the shelf-edge front associated with the western jet current along northern Brazil and the Guianas.

*Eastern Tropical Atlantic (ETRA)*—This is the zone where open-ocean algal blooms are induced by distantly-forced seasonal thermocline uplift, east of the meridional hinge line at about 20°W (Longhurst, 1993). The Angola thermal dome is located in the southeast of the province, and divergence along the equator enhances the regional, seasonal algal bloom. The boundaries may be taken as the convergence with the eastward Guinea Current to the north and the flow of the northern branch of the South Equatorial Current to the south.

*S. Subtropical gyre (SATG)*—Comprises the flow of the South Equatorial Current through the region of our computations north of 10°S to the point where its northern bifurcation runs over the shelf as the western jet current off northern Brazil and the Guianas.

*Caribbean and Gulf (CARB)*—These marginal basins, lying within the Antillean island arc, are treated together simply as a matter of convenience. Winter mixing occurs in the northern basin, the Gulf of Mexico, while the Caribbean is largely under the influence of trade winds. That we have considered these two distinct basins as constituting a single province is an example of the difficulty we face in subdividing the algal domains; because of the fractal nature of topography, we could subdivide many of our provinces, especially the coastal ones, at least as logically as we could subdivide the CARB province. For the purposes of this demonstration, we have preferred to retain a relatively small number of provinces, especially because of the problem associated with estimating chlorophyll concentration from CZCS data in coastal regions.

### *Coastal-Boundary Domain*

We follow the concept (Mittelstaedt, 1991) of a Coastal Boundary zone (which we recognize as one of the primary domains of oceanic geography) defined as those parts of the general ocean circulation where interaction with coastal topography and the coastal wind regime modify the circulation. The zone so defined is often bounded seawards by the existence of a shelf-break front, and includes both major and minor coastal upwelling regions. It is in the Coastal Boundary Domain that we are most uncertain in locating boundaries between provinces; because coastal and shelf topography introduces a fractal element into the process, subdivision can be considered equally valid at almost any spatial scale (see for example, the relatively-more-detailed partitioning of Georges Bank by Sathyendranath *et al.*, 1991); what we propose here is very largely dictated by practical considerations. Because of their complex regional geography, we do not distinguish a coastal boundary in the Boreal Polar, Caribbean or Mediterranean provinces.

*NW Atlantic (NWCS)*—Continental shelf from southern Labrador to Florida (Cape Hatteras), bounded seawards by shelf-break fronts or the limit of slope water at the north wall of the Gulf Stream.

*NE Atlantic (NECS)*—The continental shelf off NW Europe from the Barents Sea to Galicia; for the purpose of our basin-scale computation, areas east of the Greenwich meridian are ignored. Seawards generally bounded by shelf-break fronts observable in satellite imagery.

*E. Atlantic (CNRY)*—The coast from Galicia (Cape Finistera) to Cape Verde, comprising an eastern boundary current with seasonally-active upwelling cells, except from 20 to 25°N, where upwelling may occur at any season. Seawards, includes the eddy field associated with meandering flow of the Canary Current.

*Guinea (GUIN)*—Comprises the coastal flow of the Guinea Current, mostly over the continental shelf, from Senegal to the Greenwich meridian for the purposes of our computations. Local upwelling occurs at 2–7°W, and heavy dilution during the boreal summer rainy season occurs off Sierra Leone and Liberia.

*Guiana (GUIA)*—This province is occupied by the western boundary current along the northeast coast of South America, from Recife to Barbados. This current becomes a



coastal jet during the advance of the southerly monsoon during boreal summer, when instability and retroreflection occurs as unstable eddies to the north of the Amazon and off Demerara.

Our analysis of regional biological oceanography was combined with practical considerations to draft an initial set of boundaries between these 18 biogeochemical provinces. Even if we are correct that chlorophyll profiles and  $P-I$  parameters are seasonally predictable within useful limits within each of these provinces, the boundaries shown on Fig. 1 are obviously not valid for all seasons or for all data sets: as we defined them at this stage—before we examined all available observations of chlorophyll profile parameters—the boundaries were treated as an approximation, which we anticipated would require adjustment after detailed examination of the profile data. In any routine procedure for monitoring basin-scale primary production from satellite sea-surface chlorophyll, we expect the boundaries between provinces to be established concurrently both with reference to the chlorophyll field itself, and to other satellite observables.

## DATA ACQUISITION AND PROCESSING

To determine to what extent  $P-I$  and chlorophyll profile parameters are seasonally predictable within each of our proposed biogeochemical provinces, we acquired and examined as comprehensive an archive of relevant observations as possible. We obtained 7945 chlorophyll profiles from many sources (Table 1) and the results of 1862 photosynthesis–illumination experiments, performed by our colleagues in the Biological Oceanography Division, mostly in the eastern North Atlantic.

The chlorophyll profiles were fitted by a shifted Gaussian distribution function (Platt *et al.*, 1988) to obtain the following parameters: the depth of the chlorophyll peak ( $z_m$ , m), the standard deviation around the peak value ( $\sigma$ , m), the total pigment within the peak ( $h$ ,  $\text{mg m}^{-2}$ ), and the background pigment ( $B_0$ ,  $\text{mg m}^{-3}$ ). In this work, chlorophyll *a* concentration is taken as the index of biomass. Given these parameters, the biomass at any depth  $z$  can be computed as:

$$B(z) = B_0 + h/(\sigma\sqrt{2\pi}) \exp - ((z - z_m)^2/2\sigma^2). \quad (1)$$

An absolute minimum statistical requirement for fitting a four-parameter function to a data set is that there be at least six data points, so we rejected 894 profiles, specified at less than six depths. The remaining profiles were considered to be successfully fitted if the fitted curves satisfied a number of conditions.

In addition to standard checks to avoid implausibly high or low values for each parameter, we required that:  $3\sigma$  had to be less than the distance between the two sampling depths immediately above and below  $z_m$ ;  $\sigma$  had to be greater than 1 m; the parametrized pigment value at  $z_m$  should not differ from the maximum observed value by more than a factor of 2; and the unexplained variance between observed and fitted values had to be less than 15%. The risk of poorly fitted curves was high when the number of sampling depths per profile was low, close to the minimum requirement of six. After rejecting those profiles that did not meet these criteria, we were able to obtain useful parameters from 6280 of the chlorophyll profiles (Fig. 2).

Some other useful parameters can be derived from the initial set of four parameters. The following are relevant to the present study, and were also computed for each profile:

Table 1 Sources of chlorophyll profile data available for fitting to Gaussian model (table continues on following page). The number of profiles available for fitting (N) and the number of profiles successfully fitted (n) are also given

Location	Source	Format	N	n
Greenland Sea	Hirche, Bremerhaven	Disc	202	200
European arctic	Jancke, Kiel	Ber. z. Polarforschung, Alfred. Wegener Inst. (44)	93	88
Barents Sea	Rey, Bergen	Disc	627	518
Baffin Bay	BIO data archives	Data Rpt. Fish. Mar. Serv., Canada (82)	4	3
Scott Inlet	BIO data archives	Can. Data Rpt. Fish. Aquat. Sci. (213)	14	0
Can archipelago	BIO data archives	Can. Data Rpt. Fish. Aquat. Sci. (386)	17	0
Can archipelago	BIO data archives	Can. Data Rpt. Fish. Aquat. Sci. (510)	10	10
Foxe Basin	BIO data archives	Can. Data Rpt. Fish. Aquat. Sci. (385)	9	9
Hudson Bay	BIO data archives	Can. Data Rpt. Fish. Aquat. Sci. (692)	8	7
Labrador Sea	BIO data archives	Can. Data Rpt. Fish. Aquat. Sci. (577)	30	29
Labrador Sea	BIO data archives	Can. Data Rpt. Fish. Aquat. Sci. (784)	17	17
Labrador Sea	BIO data archives	Can. Data Rpt. Fish. Aquat. Sci. (760)	9	9
Jones Sound	BIO data archives	Can. Data Rpt. Fish. Aquat. Sci. (676)	3	3
Azores	BIO data archives	Can. Data Rpt. Fish. Aquat. Sci. (400)	10	10
Canary Islands	Aristegui, Las Palmas	Disc	91	59
W Mediterranean	Minas, Marseille	CNEXO, Résult. campagn. mer (8)	17	16
W Mediterranean	Minas, Marseille	CNEXO, Résult. campagn. mer (26)	7	3
W Mediterranean	Minas, Marseille	IFREMER, Campagn. océanogr. françaises (11)	89	72
W Mediterranean	Cruzado, Barcelona	Cent. Estud. A. Blanes, Inform. Tecn. (1)	31	27
NW Africa	BIO library holdings	CNEXO, Résult. campagn. mer (6)	16	13
Bay of Biscay	BIO library holdings	CNEXO, Résult. campagn. mer (9)	44	38
NW Africa	BIO library holdings	CNEXO, Résult. campagn. mer (10)	117	103
NW Africa	Jancke, Hamburg	Ber. Inst. für Meerskund., Kiel (140)	71	52
NW Africa	Barber, Beaufort	CUEA Data Reports (14)	56	49
NW Africa	Barber, Beaufort	CUEA Data Reports (18)	126	108
Portugal	BIO library holdings	CNEXO, Résult. campagn. mer (25)	60	49
NW Afr 22–28°N	Finenko, Sevastopol	Voyage ATLANT 13, data archive, disc	64	34
NE Atl	Repeta, Woods Hole	US JGOFS N. Atl. Bloom Expt., Disc	50	31
NE Atl oceanic	Veldhuis, Texel	Netherlands JGOFS N. Atl. Bloom Expt., disc	29	27
NE Atl oceanic	Lowry, Wormley	British JGOFS N. Atl. Bloom Expt., disc	500	478
NE Atl oceanic	Podewski, Kiel	German JGOFS N. Atl. Bloom Expt., disc	159	129
Celtic Sea	BIO data archives	Can. Data Rpt. Fish. Aquat. Sci. (718)	39	38
N & W of Britain	Dooley, Copenhagen	Scottish Marine Lab. and Danish data archives, disc	1178	736
NW France	BIO library holdings	IFREMER, Campagn. océanogr. françaises (1)	121	46
Off W France	BIO library holdings	IFREMER, Campagn. océanogr. françaises (6)	28	1
OWS INDIA	Williams, Plymouth	OWS INDIA data archive, disc	253	248
Grand Banks	BIO data archives	Can. Data Rpt. Fish. Aquat. Sci. (579)	4	4
Grand Banks	BIO data archives	Can. Data Rpt. Fish. Aquat. Sci. (691)	16	15
Canadian NABE	BIO data archives	Canadian JGOFS N. Atl. Bloom Expt., disc	33	33
N Sargasso	BIO data archives	Canada, JGOFS 90, JGOFS 91, WOCE 91	175	169
Nova Scotia Shelf	BIO data archives	Can. Data Rpt. Fish. Aquat. Sci. (384)	14	14
Nova Scotia Shelf	BIO data archives	Data Rpt. Fish. Marine Serv., Canada (62)	26	26
Nova Scotia Shelf	BIO data archives	Data Rpt. Fish. Marine Serv., Canada (708)	63	60

Continued

Table 1 Continued

Location	Source	Format	<i>N</i>	<i>n</i>
Nova Scotia Shelf	BIO data archives	Can. Data Rpt. Fish. Aquat. Sci. (174)	23	22
US east coast	O'Reilly, Woods Hole	Archived US east coast data, disc	127	111
Georges Bank	BIO data archives	Can. Data Rpt. Fish. Aquat. Sci. (670)	101	81
Georges Bank	BIO data archives	Can. Data Rpt. Fish. Aquat. Sci. (785)	25	24
Sargasso Sea	Marra, Palisades NY	BIOWATT 1 and 2 data archives, disc	96	93
Sargasso Sea	BIO data archives	Can. Data Rpt. Fish. Aquat. Sci. (550)	28	27
Sargasso Sea	BIO data archives	Can. Data Rpt. Fish. Aquat. Sci. (798)	15	15
Sargasso Sea	BIO data archives	Can. Data Rpt. Fish. Aquat. Sci. (732)	108	104
Transatl section	BIO data archives	Canada, JGOFS 1992 trans-Atlantic section data	72	66
US east coast	Collins, Washington	NODC—File 004, disc	1215	808
Bermuda	Michaels, Bermuda	Bermuda Atlantic Time Series, data archive, disc	136	49
Bermuda Stn	Bidigare, Honolulu	Bermuda Atlantic Time Series, data archive, disc	67	67
Caribbean	Bidigare, Honolulu	US voyages, SOLAR 17 and 19, disc	21	19
Caribbean	Muller-Karger, Miami	U. Puerto Rico, Data Rept., OHER-OTEC 80	104	95
Caribbean	BIO data archives	Can. Data Rpt. Fish. Aquat. Sci. (671)	40	39
Caribbean	Muller-Karger, Miami	Mem. Soc. Cienc. Nat. La Salle, Caracas (1965)	119	35
Equatorial Atl	Herbland, L'Houmeau	CIPREA data archives, disc	90	89
Equatorial Atl	Jancke, Hamburg	Ber. Inst. fur Meeresk., Kiel (110)	191	187
Equatorial Atl	Herbland, L'Houmeau	ORSTOM expeditions FOCAL and PIRAL, archives, disc	539	525
SE Atlantic 12°S 20°W	Finenko, Sevastopol	Voyage ATL 7 data archives, disc	50	6
Guinea Dome	BIO library holdings	CNEXO, Résult. campagn. mer (13)	75	73
Gulf of Guinea	BIO library holdings	CNEXO, Résult. campagn. mer (19)	173	164
Total profiles available for fitting 7945				
Total profiles successfully fitted 6280				

The height  $H$  of the peak above the background can be derived from  $h$  and  $\sigma$ :  $H = h/(\sigma\sqrt{2\pi})$ .

The ratio of peak height to total pigment at  $z_m$  ( $\rho' = H/(H + B_0)$ ). (Note:  $\rho'$  is different from  $\rho$  used by Sathyendranath and Platt (1989) and Platt *et al.* (1991):  $\rho = H/B_0$ . While both  $\rho$  and  $\rho'$  can be used to define the relative importance of the peak compared to the background,  $\rho'$  is mathematically more convenient to use:  $\rho = H/B_0$  would go to infinity if  $B_0$  were zero, while  $\rho' = H/(H + B_0)$  is confined to the range 0 to 1.)

To examine how the surface chlorophyll is related to the rest of the profile, we also needed  $B(0)$ , which was derived from (1) by setting  $z = 1$ .

To evaluate how the oceanographic differences in the provinces are reflected in the structure of the chlorophyll profiles and algal physiology, we binned both the  $P-I$  and the chlorophyll-profile parameters by province and by season, for further statistical analysis.

## CONFIRMATION OF BOUNDARIES BETWEEN PROVINCES

Because the subsurface peak in chlorophyll is one of the most consistent features of algal distribution in the ocean and responds directly to differences in regional oceanography

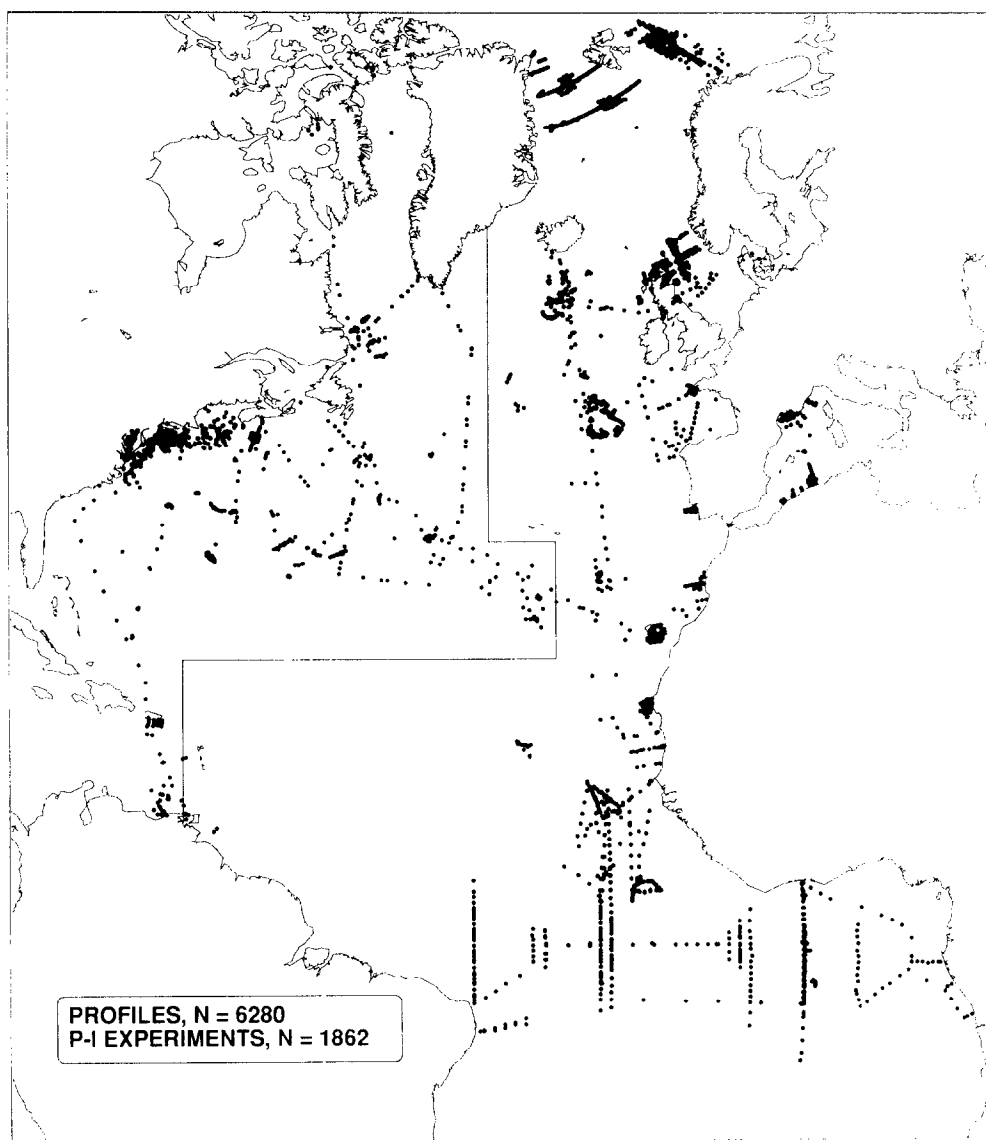


Fig. 2. Station positions of the 6280 chlorophyll profiles for which an adequate fit to the Gaussian model was obtained. The 1862  $P-I$  experiments used in this study were all performed to the west of the line shown on the map.

(Yentsch, 1965; Venrick, 1988), we used the values of  $z_m$  to check that our choice of boundaries between the provinces was appropriate. We found that, within provinces, a few of the seasonal frequency distributions of  $z_m$  were bimodal, suggesting that the boundaries of the compartments had been improperly drawn. In each case, we found that the minor mode was usually caused by a group of profiles from a single cruise or experiment which lay across one of the originally selected boundaries; in such cases it was found that a minor readjustment of the boundary resolved the bimodality.

The clearest case was that of the data binned into the NWCS, which included several hundred profiles from within Chesapeake Bay having very shallow values of  $z_m$ . This caused the whole bin to be strongly bimodal; this was resolved by creating a separate compartment (CHSB), presumed to be characteristic of the inner neritic regions and which we identified separately in our computations.

Similarly, the data sets from the UK and Netherlands JGOFS 89 voyages created bimodality within the STGE province to which they were first assigned. Since their values fitted those of the NADR province, to which they were closely adjacent, a minor alteration to the relevant boundary resolved the problem. Similarly, a number of profiles from off Puerto Rico were anomalous in the NATR province to which they were first allocated, and their transfer to the CARB province, when it was realized they were on the southern side of the island, removed the anomalous minor peak in the NATR province.

We found that bimodal distributions of  $z_m$  in the subtropical and tropical parts of the gyre indicated a discontinuous distribution of data between the eastern (shallower) and western (deeper) thermocline situations. We could, however, find no natural discontinuity on which to locate a meridional boundary in the tropical gyral province, as we have (see previous section) for the subtropical part of the gyre (STGW and STGE) and for the tropical region (WTRA and ETRA).

When we were satisfied that the boundaries fitted the data as well as we could manage subjectively, we computed descriptive statistics for each parameter for each (province, season) case. We were thus able to derive a set of parameter values representing 65 of the possible 76 cases (19 provinces, 4 seasons). The remaining 11 cases, for which we had no profiles, were dealt with in our final computations by using values for the missing season from adjacent provinces, or for another season in the same region, whichever conformed better to our knowledge of regional oceanographic processes.

## SIGNIFICANCE OF BOUNDARIES BETWEEN PROVINCES

Our final check that the boundaries were realistic was to investigate statistically the differences between seasonal mean parameter values for adjacent provinces. Since, in the approach of Platt and Sathyendranath (1988) to remote sensing of primary production,  $z_m$ ,  $\sigma$  and  $\rho'$  are the parameters that are to be used in conjunction with surface chlorophyll from satellite data, we restricted our analysis to these three parameters.

We found that the differences in the depth of the chlorophyll maximum ( $z_m$ ) between adjacent provinces are significant at the 5% level for 36 cases out of 99 (Fig. 3), with the differences being most pronounced in summer (50% of the cases), and least in winter (25%). The differences were significant in only 10 cases out of 99 for  $\sigma$ , and for seven cases for  $\rho'$ .

We found that, for all three parameters, the most consistent boundary zones are between the coastal and oceanic domains, while between the oceanic provinces the most distinct boundaries lie to the north and south of the subtropical gyre, that is, north of the Azores Current and south of the subtropical convergence zone. Most boundaries between oceanic provinces prove to have some significance for  $z_m$ , and this parameter also confirms the reality of the east–west partition of both the subtropical gyre (STGW/STGE) and of the tropical Atlantic (WTRA/ETRA). The depth of the chlorophyll maximum in the SATG and CARB also reflects the deeper mixed layers, compared with the tropical

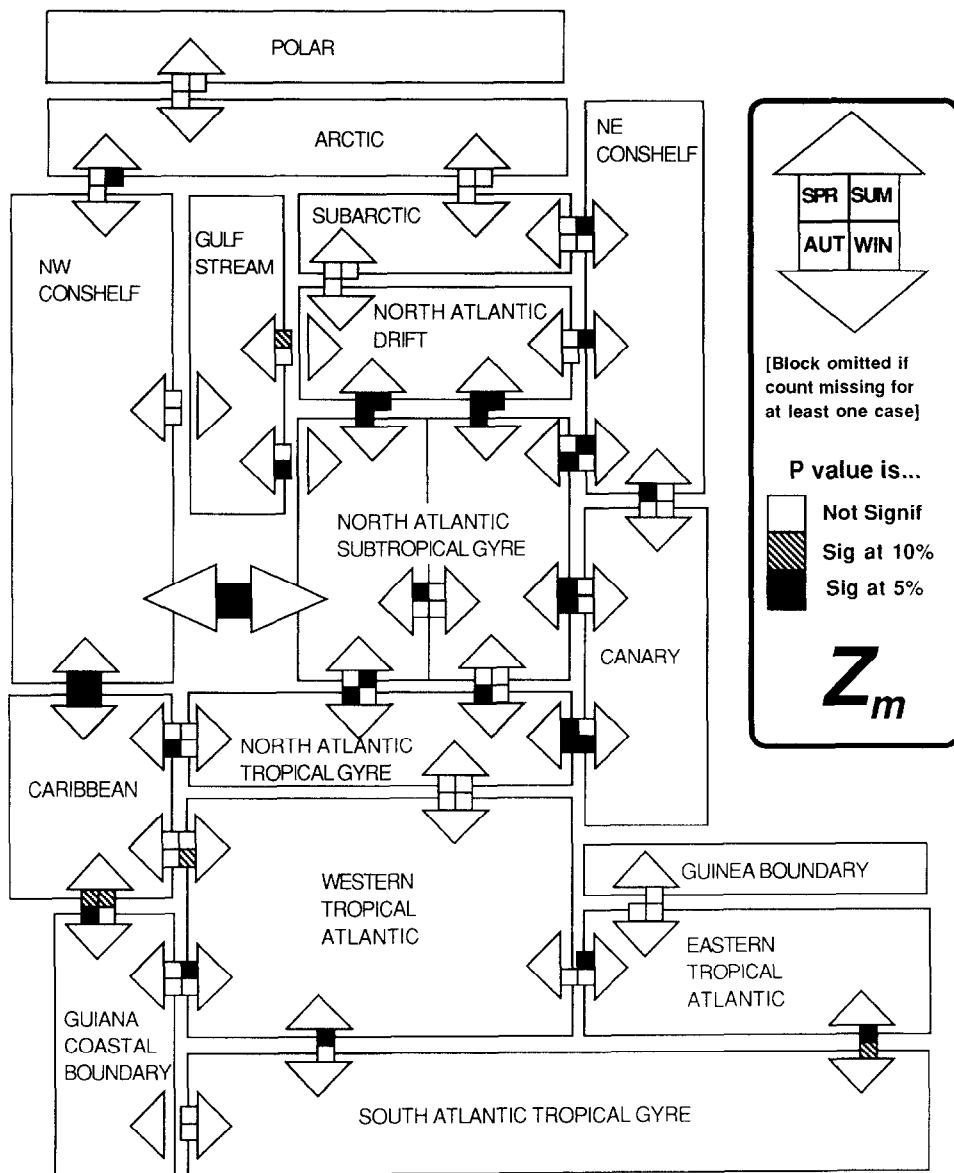


Fig. 3. Diagram analysing the differences of the parameter  $z_m$ , seasonally, between adjacent provinces, shown as the significance (P) of the ANOVA Bonferroni-Dunn post-hoc test (Miller, 1966). Note that the orientation of the four blocks representing seasonal significance remains as shown in the legend for both vertically and horizontally oriented icons.

oceanic provinces NATR, WTRA and ETRA, which have shallower mixed layers and shallower chlorophyll maxima.

For  $\rho'$ , differences across oceanic province boundaries are slight, for all seasons and from polar to tropical regions: for this parameter, the principal distinction is between

coastal and oceanic domains. The parameter  $\sigma$  is a somewhat intermediate case, following the pattern of  $z_m$ , but less clearly.

The most striking failure of these parameters to respond to the boundaries between provinces occurs in the north. Poleward of the bifurcation of the Gulf Stream into a northeasterly North Atlantic Current and a southeasterly Azores Current, differences between provinces of the seasonal depth of the chlorophyll maximum ( $z_m$ ) are slight, though there are differences in  $\sigma$  in spring across the NADR/SARC and SARC/ARCT boundaries. The distribution of parameters of the chlorophyll profile do not, therefore, support our proposal that the existence of a superficial brackish layer north of the Oceanic Polar Front will lead to a fundamental change in the dynamics of the spring bloom along this boundary. The difference is one of timing, not chlorophyll profile structure.

Next we discuss the use of parameters of the chlorophyll profile to check that there are characteristic differences between seasonal algal growth dynamics (as expressed in the distribution of chlorophyll) representative of individual biogeochemical provinces, and that such differences are not counter-intuitive.

Because dynamics of algal growth differ strongly between regions of the ocean, we had little confidence in seasonality of global parameters, so we also investigated to what extent characteristic seasonal cycles were demonstrated in our set of provinces. At least the sign of some of the seasonal changes we found (Fig. 4) would have been predictable from general knowledge of seasonal cycles of algal growth in the ocean. For instance, we find that:

The depth of the chlorophyll maximum  $z_m$  becomes progressively greater from spring to fall in the open ocean in mid-latitudes (NADR, STGW, STGE, NWCS), and the thickness of the subsurface chlorophyll layer (indicated by  $\sigma$ ) in SARC, STGW, NATR, NWCS, NECS, and CNRY becomes thinner during the summer and autumn, compared with winter.

The parameter  $z_m$  shoals and there is a concomitant increase in the slope of the peak ( $H/\sigma$ ), from summer to winter in the ETRA compared with the western tropical ocean (WTRA). Such differences between provinces support the view that it is preferable to partition basin-scale computations of primary production rather than treating all pixels in the entire basin as belonging to the same statistical population.

Finally, we extended this part of our investigation by inspecting the relative variance of means for the chlorophyll parameter values, for all provinces and seasons, to assess the confidence that could be placed in their individual means (Fig. 5). We found that the means of all parameters for low-latitude oceanic provinces have lower variance than mid to high latitudes and the coastal boundary regions (Table 2). We suggest that this result is a consequence of the relatively greater vertical stability of the water column in the tropics than in subtropical and temperate zones.

## SURFACE CHLOROPHYLL AS A PREDICTOR OF SUBSURFACE STRUCTURE

We are now in a position to return to the question of whether surface chlorophyll  $B(0)$  is a sufficient predictor of the form of the chlorophyll profile for present purposes, as suggested by Morel and Berthon (1989). It is desirable that the form of the chlorophyll profile be parametrized in one way or another, for an assumption of a uniform chlorophyll profile whose pigment concentration was specified by its surface value could lead to

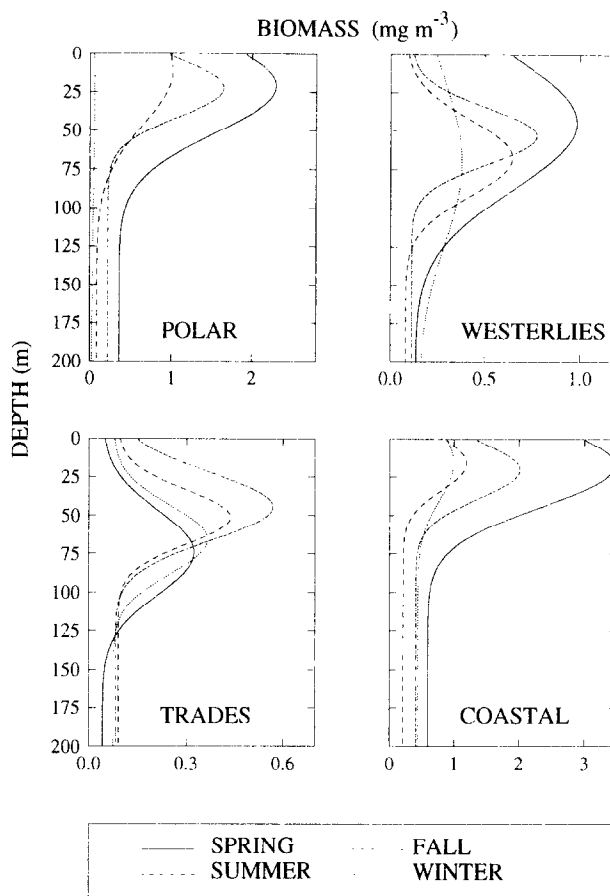


Fig. 4. Mean fitted profiles for four seasons in the four primary biogeochemical domains.

inaccurate estimates of integrated primary production. This problem was examined from a theoretical point of view by Platt *et al.* (1988) and by Sathyendranath *et al.* (1989), who showed that the errors depended on dimensionless numbers such as the ratio of  $z_m$  to the photic depth  $z_p$ . We return to this question later.

Analytical models of primary production require depth-dependent values of chlorophyll, rather than an integrated chlorophyll concentration. This is another reason to examine whether the surface chlorophyll concentration predicts the other parameters that define the chlorophyll profile. Reflecting the global relationship between surface and integrated chlorophyll from actual profiles, our data confirm that surface chlorophyll predicts some aspects of the subsurface form of the chlorophyll profile itself (Table 3), though the relationships between  $B(0)$  and the parameters of the profile are, at best, somewhat weak.

For all provinces and seasons combined, the relationship between  $B(0)$  and depth of the sub-surface chlorophyll maximum ( $z_m$ ) takes a value of Spearman's  $\rho$  of  $-0.623$ , while for  $\sigma$ , Spearman's  $\rho$  is  $0.116$ , suggesting that prediction of this parameter from surface chlorophyll is impracticable. For the 16 cases representing the four algal domains in all



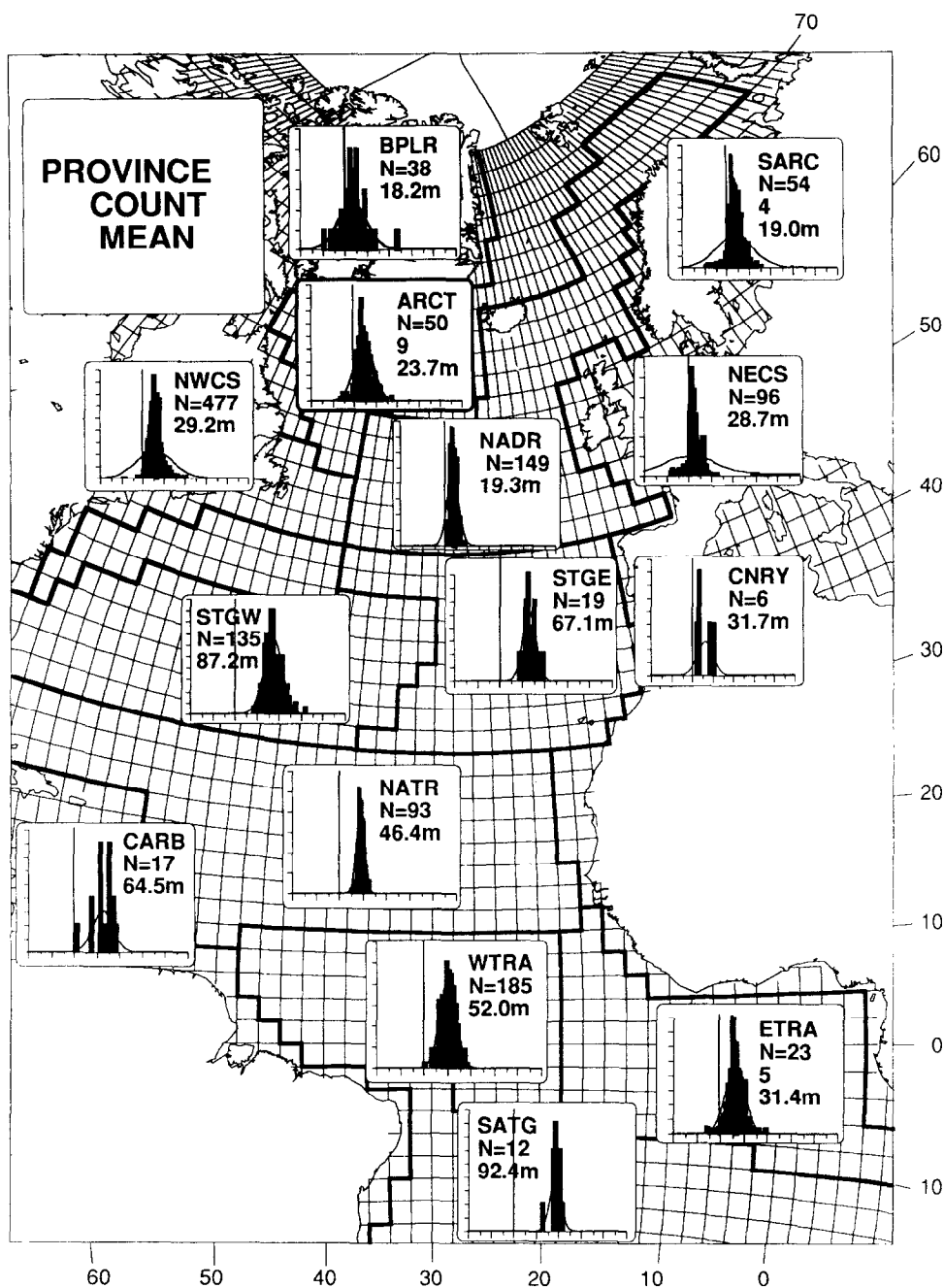


Fig. 5. Map to show the layout of the provinces on a  $2^{\circ} \times 2^{\circ}$  degree grid of the North Atlantic Ocean, for the final computation of basin-scale primary production. Also shown are exemplary frequency histograms of  $z_m$  for the summer season, for many of the provinces. Scales adjusted to fit the data, the vertical line in each graph indicating the locations of  $z_m = 0$  m. A normal curve is fitted to each distribution.

Table 2. Annual means and variance of computed euphotic depths and parameters of the chlorophyll profiles for individual provinces grouped by primary ecological domains. Note that the euphotic zone is calculated even for coastal provinces assuming case 1 waters, and so the estimated photic depths can differ significantly from the real case. This would be particularly true of the Chesapeake Bay. Note also, that in the coastal waters the hypothetical photic depth computed may be greater than the actual station depth. The parameters  $z_p$ ,  $z_m$  and  $\sigma$  are in m and  $\rho$  is dimensionless

Regions	Count	Mean $z_p$	CV	Mean $z_m$	CV	Mean $\sigma$	CV	Mean $\rho$	CV
Polar domain									
BPLR	73	33	0.42	15	1.9	18	0.9	0.83	0.23
ARCT	622	40	0.33	23	1.0	18	0.8	0.87	0.19
SARC	990	39	0.35	19	2.1	28	1.1	0.84	0.23
Westerlies domain									
NADR	426	38	0.21	16	1.5	19	0.8	0.87	0.19
GFST	50	38	0.28	47	2.9	35	1.6	0.91	0.16
STGE	188	59	0.24	56	1.2	33	1.2	0.81	0.23
STGW	459	64	0.23	84	0.9	51	1.7	0.85	0.20
MEDI	115	58	0.21	49	0.4	17	0.8	0.85	0.15
Trades domain									
NATR	212	60	0.14	49	0.6	13	1.4	0.85	0.10
CARB	140	76	0.13	77	0.6	32	0.9	0.87	0.15
WTRA	441	65	0.13	57	0.3	25	0.5	0.88	0.13
ETRA	383	57	0.15	37	0.5	20	0.6	0.83	0.20
SATG	27	79	0.05	95	0.2	19	0.6	0.73	0.13
Coastal domain									
NECS	520	35	0.28	14	4.2	28	1.6	0.73	0.37
CNRY	385	31	0.33	10	4.8	29	1.1	0.83	0.29
GUIN	16	55	0.22	32	0.6	15	0.8	0.91	0.08
NWCS	895	39	0.34	25	1.7	19	2.0	0.82	0.25
GUIA	37	69	0.28	53	1.6	33	1.2	0.72	0.35
CHSB	301	78	0.17	2.5	15	12	2.0	0.59	0.44
North Atlantic basin									
	6280	48	0.23	31	0.6	25	0.5	0.82	0.003

seasons, Spearman's  $\rho$  between  $B(0)$  and  $z_m$  ranges from  $-0.026$  to  $-0.832$ , with the winter season in coastal areas not unexpectedly yielding the very lowest value. For  $B(0)$  and  $\sigma$ , the correlation in coastal waters is clearly erroneous, yielding low positive values for all seasons; the highest values of  $\rho$  for this relationship occur in summer, when subsurface maxima are expected to be isolated from the surface, and  $\rho$  reaches values of approximately  $\pm 0.3$  in each of the oceanic domains.

These results support the view that a spatially-realistic distribution in the computed field of primary production is more likely to be achieved with an assignment of parameters for the chlorophyll profile made on a province-to-province basis rather than one derived from a universal relationship that uses surface chlorophyll as a proxy for profile shape.

## VARIABILITY OF THE $P$ - $I$ PARAMETERS

The spatial distribution of available  $P$ - $I$  data is less satisfactory than that of chlorophyll profiles, even when the data are partitioned into the four primary domains (Table 4, and

Table 3. Surface chlorophyll  $B(0)$  as a predictor of parameters ( $z_m$  and  $\sigma$ ) of the chlorophyll profile, as indicated by Spearman's ranked correlation ( $\rho$ ) for seasons in primary domains, and for provinces, annually

Season	$N$	$z_m B(0)$	$\rho$ $\sigma B(0)$	Province	$N$	$z_m B(0)$	$\rho$ $\sigma B(0)$
Polar domain							
Spring	489	-0.36	-0.15	BPLR	73	-0.52	0.22
Summer	1091	-0.56	0.31	ARCT	622	-0.48	0.21
Autumn	92	-0.49	-0.14	SARC	990	-0.47	0.12
Winter	13	-0.24	0.37				
Westerlies domain							
Spring	662	-0.73	-0.07	NADR	426	-0.58	0.22
Summer	391	-0.83	-0.26	GFST	50	-0.71	0.03
Autumn	141	-0.71	-0.15	STGE	188	-0.68	0.24
Winter	44	-0.77	-0.03	STGW	459	-0.53	0.36
				MEDI	115	-0.54	-0.04
Trades domain							
Spring	182	-0.33	-0.09	NATR	212	-0.12	-0.32
Summer	542	-0.72	0.30	CARB	140	-0.45	0.07
Autumn	237	-0.55	-0.13	WTRA	441	-0.48	0.09
Winter	242	-0.40	-0.31	ETRA	383	-0.71	0.36
				SATG	27	-0.24	-0.54
Coastal domain							
Spring	791	-0.34	0.24	NECS	520	-0.39	0.08
Summer	863	-0.44	0.28	CNRY	385	-0.41	0.08
Autumn	390	-0.15	0.27	GUIN	16	-0.68	0.22
Winter	110	-0.03	0.04	NWCS	895	-0.59	0.24
				CHSB	301	-0.26	-0.15
				GUIA	37	-0.49	-0.07
				North Atlantic basin	6280	-0.62	0.12

the distribution of  $P$ - $I$  stations shown in Fig. 2). The situation is even less satisfactory for individual provinces: of 1862 sets of  $P$ - $I$  parameters, only 133 are not within five northwest Atlantic provinces—BPLR, ARCT, GFST, STGW and NWCS. Nor is the distribution among primary domains fully satisfactory, with the tropical region being undersampled: Polar—599 experiments; Westerlies—422; Coastal—818; and Trades—only 23.

This would be a serious difficulty if there were not consistently greater variability in observations of phytoplankton pigments than in measurements of the rate processes associated with its growth (Platt and Sathyendranath, 1988): for the data base used here, the dynamic range of mean values (max/min) between cases (domains, seasons) is 4.3 for  $\alpha^B$  and 3.2 for  $P_m^B$ .

In the mid-latitude oceanic regions, where most of our data come from the Sargasso Sea, we find that  $P_m^B$  is more sensitive to depth than  $\alpha^B$ , which is relatively invariant (Note, however, that  $\alpha^B$  does show a strong depth dependence during summer, stratified months, see Platt *et al.*, 1992). This difference between the sensitivity of the two parameters to depth is maintained in both the Polar and the better-mixed and shallower Coastal areas, though in both of these the change of  $P_m^B$  with depth is less strong than in the Sargasso Sea.

Table 4. Distribution of P-I experiments by domain and season, and the variance of the estimated photosynthetic parameters. The parameter  $\alpha^B$  is in  $\text{mg C (mg Chl)}^{-1} \text{h}^{-1} (\text{W m}^{-2})^{-1}$  and  $P_m^B$  is in  $\text{mg C (mg Chl)}^{-1} \text{h}^{-1}$

Domain	Season	N	Mean	$\alpha^B$		Mean	$P_m^B$	
				SD	CV		SD	CV
North Atlantic Polar	Total	1862	0.11	0.10	0.85	3.2	2.3	0.7
	Spring	60	0.10	0.05	0.47	2.5	0.9	0.4
	Summer	437	0.11	0.09	0.82	2.1	1.5	0.7
	Autumn	74	0.09	0.05	0.57	1.6	0.7	0.5
	Winter	28	0.11	0.04	0.36	2.1	0.8	0.4
Westerlies	Spring	313	0.11	0.04	0.41	5.0	2.6	0.5
	Summer	80	0.06	0.03	0.55	1.7	1.6	0.9
	Autumn	21	0.06	0.03	0.53	2.6	1.5	0.6
	Winter	8	0.11	0.04	0.36	3.7	1.8	0.5
Trades*	Winter	23	0.14	0.13	0.92	3.4	2.5	0.7
Coastal	Spring	306	0.11	0.07	0.67	2.8	1.2	0.4
	Summer	363	0.14	0.15	1.04	3.6	2.7	0.8
	Autumn	58	0.24	0.17	0.70	5.0	2.4	0.5
	Winter	91	0.12	0.10	0.81	3.0	1.2	0.4

\*We did not feel that these few observations from the eastern Caribbean and off Florida could be taken to be representative of all trade-wind domains. Therefore, the following numbers were used in the trades for all seasons:  $\alpha^B = 0.055 \text{ mg C (mg Chl)}^{-1} \text{h}^{-1} (\text{W m}^{-2})^{-1}$  which is assumed to be typical of low-nitrate, low-biomass, warm waters, based on the results of Platt *et al.* (1992), and  $P_m^B = 4 \text{ mg C (mg Chl)}^{-1} \text{h}^{-1}$  (if we take noon surface irradiance in the tropics to be  $\sim 400 \text{ W m}^{-2}$ , then from Fig. 2 of Platt and Sathyendranath (1993) we get  $I_k \sim 70 \text{ W m}^{-2}$ , and with  $P_m^B = I_k \alpha^B$ , we have  $P_m^B \sim 4$ ).

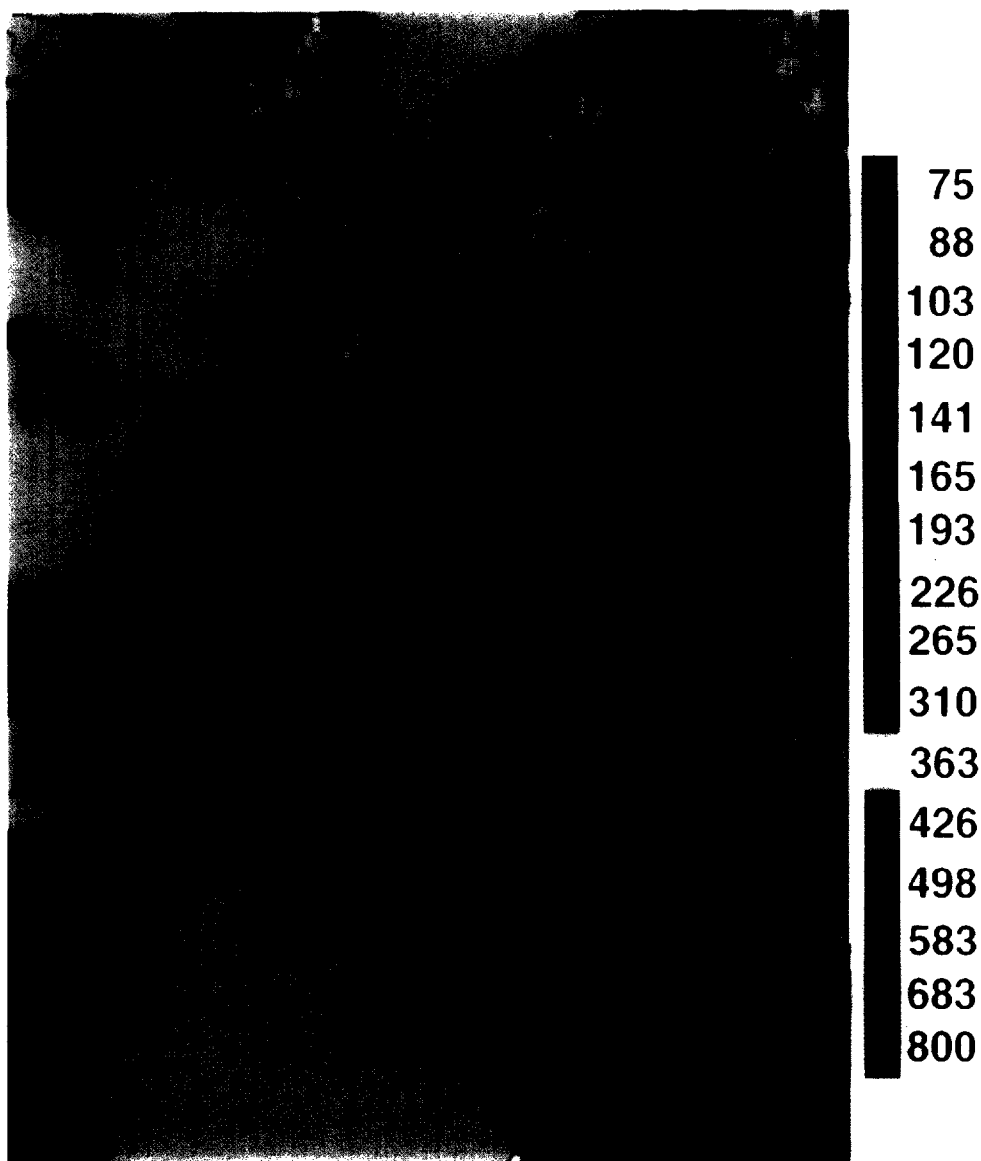
Although coherent seasonal changes in  $\alpha^B$  can be followed where the data are sufficient, as in the Westerlies data from the Northern Sargasso Sea, this is more difficult in the Coastal and Polar data, which are more heterogeneous environments, and where the seasonal changes are compromised by the effect of local conditions in experimental areas. The regional, seasonal mean values (Table 4) reflect these differences.

## COMPUTATION OF PRIMARY PRODUCTION FOR THE NORTH ATLANTIC BASIN

### *Selection and application of local algorithm*

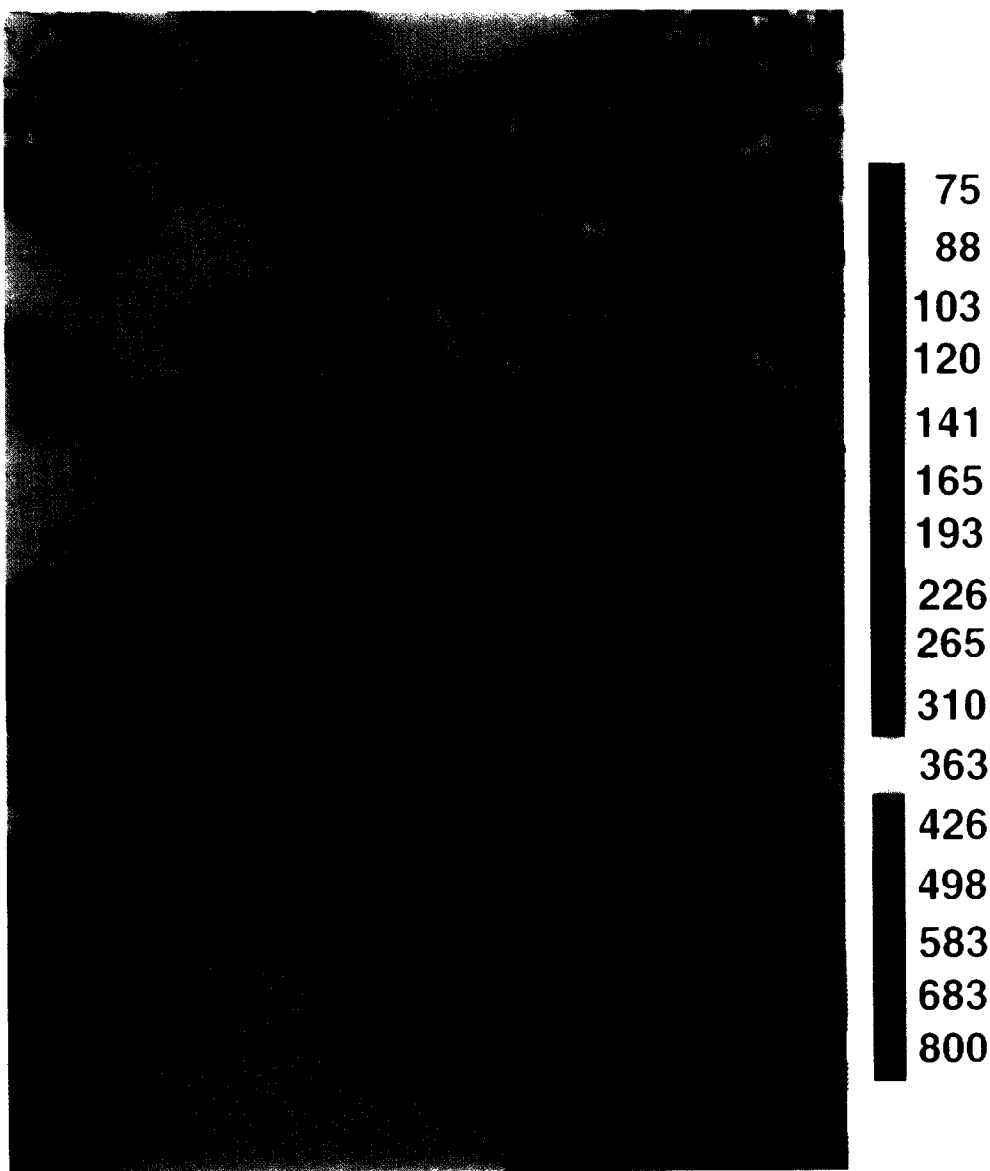
In this section, we present a computation of primary production for the North Atlantic from  $89^\circ\text{W}$  to  $1^\circ\text{E}$  and  $10^\circ\text{S}$  to  $70^\circ\text{N}$ , differentiated by four seasons and 19 biogeochemical provinces (the area for which the computations are carried out differs slightly from that of Platt *et al.*, 1991).

Primary production was computed for each month (represented by the 15<sup>th</sup> of the month) for each  $1^\circ$  grid in the study area and integrated to annual production. The seasonal mean values of  $z_m$ ,  $\sigma$  and  $\rho'$  were used along with monthly, ocean-colour data for 1979 to derive the chlorophyll profile at each pixel, using the approach of Sathyendranath and Platt (1989), modified to use  $\rho'$  instead of  $\rho$ . Correction for cloud cover was applied as in Platt *et al.* (1991). If there were missing ocean-colour pixels in any month, those pixels



**ESTIMATED PRIMARY PRODUCTION 1979  
BASED ON BIOGEOCHEMICAL PROVINCES**  
( g C m<sup>-2</sup> y<sup>-1</sup> )

Fig. 6. Estimated primary production for the North Atlantic Ocean computed as described in the text for the year 1979; model parameters are partitioned by biogeochemical provinces outlined in the present study.



**ESTIMATED PRIMARY PRODUCTION 1979  
BASED ON LATITUDINAL ZONES**

**( g C m<sup>-2</sup> y<sup>-1</sup> )**

Fig. 7. Estimated primary production for the North Atlantic Ocean computed as described in the text for the year 1979, for comparison with Fig. 6; in this computation, the model parameters are partitioned by the latitude and depth compartments used by Platt *et al.* (1991).

were assigned production values corresponding to the monthly-means for the province in which the missing value occurred.

The local algorithm of Platt *et al.* (1991) was used in the present computation with the following modifications: (i) the light available at depth was computed every 0.5 m instead of every 1 m; (ii) the computations were repeated for 12 time intervals from dawn to local noon (assuming symmetry around local noon) according to Platt and Sathyendranath (1991); (iii) two linear equations (Prieur and Sathyendranath, 1981) having a discontinuity at  $1 \text{ mg m}^{-3}$  were used for computing light absorption by phytoplankton at 440 nm rather than the equation of Sathyendranath and Platt (1988), which is not applicable to biomass greater than  $10 \text{ mg m}^{-3}$ ; and (iv) finally, the computed photic depth was checked against a bathymetry file and integration terminated either at the indicated bottom of the water column or at the photic depth (the photic depth  $z_p$  was computed as that depth at which the integrated daily light was reduced to 1% of the integrated surface light). The check against bathymetry reduced the computed primary production at some coastal pixels, whereas the change in the computation of phytoplankton absorption reduced the photic depth and the production at high-biomass stations.

We compared the performance of the modified local algorithm with the original local algorithm of Platt *et al.* (1991), by repeating the basin-scale computations for the same input files using both the local algorithms, and found that the overall effect of the modifications is a reduction in computed, annual, basin-scale production of about 23%.

The computed primary-production in the N. Atlantic basin for 1979 is shown in Fig. 6. The contributions from the 19 provinces are listed in Table 5. If the computations are extended to the 0.1% light level, then the estimated primary production for the basin would increase from 10.5 to  $10.7 \text{ Gt C y}^{-1}$ . To evaluate the impact of extrapolation schemes on the results of large-scale computations, we next compare these results against those obtained for other extrapolation schemes.

#### *Effect of using bio-geographical provinces rather than latitudinal regions*

To examine the effect of using a geographic partition of the basin into 19 provinces rather than the 12 latitudinal regions used by Platt *et al.* (1991), we repeated the computations using the Platt *et al.* (1991) partition. To ensure that the differences seen in the results arise only from the way the basin was partitioned, and not from the improved data archive used for defining the parameter field, nor from changes to the local algorithm used by Platt *et al.* (1991), the new data archive presented here was used to compute the seasonal, provincial parameter fields for the Platt *et al.* (1991) regions as well. The distribution of annual production obtained for the partitioning scheme of Platt *et al.* (1991) is shown in Fig. 7.

At the scale of the entire basin, the results for annual primary production differ little between the two cases:  $10.5 \text{ Gt C y}^{-1}$  for the new partition into provinces, and  $9.9 \text{ Gt C y}^{-1}$  for the earlier partition into latitudinal regions. However, the spatial distribution of the primary production for the calculation based on provinces appeals much more to the oceanographic intuition than does that based on a partition into latitudinal regions (Figs 6 and 7). It is not straightforward to compare the two results at the scale of the provinces, since the 12 latitudinal regions and the 19 provinces cannot be matched on a one-for-one basis. So, for that calculation based on latitudinal regions, the production in each province was obtained as the sum of the values for those portions of each latitudinal region that are

Table 5. Comparison of basin-scale computation of North Atlantic primary production partitioned by the suite of biogeochemical provinces described in this study, and by the latitudinal zones used by Platt *et al.* (1991). For the biogeochemical provinces, results of computations using uniform and non-uniform profiles are given. For the computations based on latitudinal zones as well as for those based on uniform profiles, the percentage differences compared to our best calculations (the biogeochemical provinces, non-uniform-biomass case) are given. Each computation was performed using the updated local algorithm described in the text. Units are  $\text{gC m}^{-2}$  and  $\text{GtC per year}$

		Biogeochemical Provinces					Latitudinal Zones		
	Area	Non-Uniform		Uniform			Non-Uniform		
	(10 <sup>6</sup> km <sup>2</sup> )	annual prod.	(GtC)	annual prod.	(GtC)	Diff.	annual prod.	Diff.	
		(gCm <sup>-2</sup> )		(gCm <sup>-2</sup> )		%	(gCm <sup>-2</sup> )	%	
<hr/>									
Polar domain									
BPLR	2.14	526	1.13	507	1.09	3.6	341	0.73	35.4
ARCT	2.44	319	0.78	289	0.71	9.4	323	0.79	-1.3
SARC	1.04	307	0.32	296	0.31	3.6	322	0.34	-6.3
Total			2.23		2.11			1.86	
Westerlies domain									
NADR	3.50	243	0.85	230	0.81	5.3	317	1.11	-30.6
GFST	1.10	175	0.19	154	0.17	12.0	244	0.27	-42.1
STGW	5.80	103	0.60	96	0.55	6.8	114	0.66	-10.0
STGE	4.45	137	0.61	126	0.56	8.0	174	0.77	-26.2
MEDI	0.148	269	0.04	218	0.03	19.0	180	0.03	25.0
Total			2.29		2.12			2.84	
Trades domain									
NATR	8.27	123	1.01	105	0.87	14.6	122	1.01	0.0
WTRA	5.36	123	0.66	103	0.55	16.3	120	0.64	3.0
ETRA	3.91	146	0.57	131	0.51	10.3	150	0.59	-3.5
CARB	3.58	218	0.78	188	0.67	13.8	162	0.58	25.6
SATG	1.13	66	0.07	65	0.07	1.5	79	0.09	-28.6
Total			3.09		2.67			2.91	
Coastal domain									
NECS	0.624	648	0.40	640	0.40	1.2	514	0.32	20.0
CNRY	0.813	691	0.56	650	0.53	5.9	600	0.49	12.5
GUIN	0.491	562	0.28	484	0.24	13.9	346	0.17	39.3
GUIA	1.23	466	0.57	454	0.56	2.6	335	0.41	28.1
NWCS	2.00	509	1.02	431	0.86	15.3	462	0.92	9.8
CHSB	0.0199	1278	0.03	1270	0.03	0.6	982	0.02	33.3
Total			2.86		2.62			2.33	
North Atlantic basin									
Total			10.5		9.5			9.9	

contained within the boundaries of the province. These results (Table 5) show that the agreement at the basin scale is a fortuitous consequence of self-cancelling by positive and negative differences that range from -42 to +39%.

Conceptually, the partitioning of the ocean basin into biogeochemical provinces, based rationally on known features of Atlantic oceanography and ecology, is more satisfying than the simpler partitioning according to latitude and depth which was used as an illustration, by Platt *et al.* (1991), simply because we can be confident that those boundaries do not reflect natural discontinuities. Besides, the biogeographic provinces, as we have defined them here, have characteristic (and intuitively correct) chlorophyll profiles. However, we do not pretend that this is the only possible approach for



computation of primary production at large scales. We go no farther than suggesting that such a scheme should be given strong consideration for operational monitoring of primary production from the sea-surface chlorophyll field, to the extent that it is practicable.

### *Effect of chlorophyll-profile parameters*

The results of Platt *et al.* (1991) suggested that primary production computed from uniform profiles differed from that based on non-uniform profiles by  $\leq 20\%$ . They cautioned, however, that this was probably an exaggerated effect because the light-transmission model used was overestimating the light at depth, for high-biomass pixels. The change in the parametrization of light absorption described for the present computations was designed to reduce this error by increasing the attenuation coefficient for high chlorophyll concentrations. Consequently, a relative decrease in primary production at depth will be indicated, making the model less sensitive to changes in deep-chlorophyll maxima. In this section we examine the impact of non-uniform profiles on large-scale primary production, using the improved local algorithm.

The effect of including information on the vertical distribution of chlorophyll is, in general, to increase the estimate of primary production. To show this, we made a further calculation in which the chlorophyll was considered to be uniformly distributed with depth. The relative difference between the result of this calculation and that where the chlorophyll was considered nonuniform provides an index of the importance of taking the chlorophyll profile into account. At the scale of the individual provinces, the non-uniform result was always equal to or higher than the uniform one (Table 5). At the basin scale, the two calculations differed by some 9%, though higher differences do exist at the scale of the provinces. (Note that, if the computations were carried out to the 0.1% light level instead of the 1% level, this would lead to an increase of  $0.2 \text{ Gt C y}^{-1}$  in the computed primary production for the uniform case, similar to the results obtained for the non-uniform case.) For the Arabian Sea, Brock *et al.* (1993) suggested that deep-chlorophyll maxima contribute significantly to the water-column production during periods of low biomass and, therefore, low productivity. Such a simple conclusion would not be appropriate for the N. Atlantic, since we were not able to correlate the effect of non-uniformity (estimated as relative difference between computations for uniform and non-uniform cases for a given month and a given province) with the level of primary productivity.

One could also examine the effect of the enlarged data set of chlorophyll profiles used in this study, compared to the one used by Platt *et al.* (1991). In fact, if the computations based on the latitudinal regions are repeated with the older set of chlorophyll-profile parameters, one obtains a basin-scale production of  $10.4 \text{ Gt C y}^{-1}$ , compared to  $9.9 \text{ Gt C y}^{-1}$  obtained from the new set of parameters and the latitudinal partition. In other words, at the basin scale, the net effect of increasing the number of chlorophyll profiles in the data base used is to narrow the gap between the results of this calculation and that in which the chlorophyll would be considered to be uniformly distributed with depth.

The parameters describing the chlorophyll profile define the depth and shape of the subsurface chlorophyll maximum, when it is present. An increase in biomass at depth, in the light-limited part of the water column, may not have the same impact on primary production as a similar increase at the surface. So the effect of deep chlorophyll maxima can be considered a second-order effect on primary production compared to changes in

surface biomass or surface irradiance, both of which can, fortunately, be monitored directly by satellites. In fact, the differences between the uniform-profile case and the non-uniform cases are small, at least for the annual, basin-scale computations. Given that deep chlorophyll maxima have a relatively small impact on computed primary production compared to other greater uncertainties that exist in the computational procedures, one might argue that it is premature to worry at all about non-uniformity in vertical structure, at least until the other errors have been addressed.

But there are some counter-arguments to this reasoning: (i) Subsurface chlorophyll maxima are a consistent feature in the oceans. Generally, accounting for their presence increases estimates of integrated primary production; so ignoring them will affect not the precision, but the accuracy of the estimates. Since this error is systematic, the results will remain biased, even when averaged over several pixels. (ii) In climate-related studies, it is important to know not just the gross primary production (as in the present computations), but the new production (nitrate-driven production) as well. If we consider that the production which is exported out of the mixed layer constitutes new production, and that the deep chlorophyll maxima appear below the mixed layer, then it would be likely that most of the primary production in the deep chlorophyll maxima is new production. It may well be that, when the focus is shifted from total to new production, the relative importance of the deep chlorophyll maxima would increase. One cannot study problems such as this unless the models are able to deal with non-uniform profiles. (iii) If these computations are to be used in the context of a changing climate, one of the questions to be addressed would be whether there are any trends in large-scale primary productivity of the oceans, at the annual scale. If such trends do exist, they are likely to be small, and approaches that choose to ignore small, but systematic errors would not be particularly suitable for such exercises. So it is premature to accept the easier solution of computing and monitoring basin-scale primary production with minimalist models based on a uniform-chlorophyll profile.

However, if computed primary production is relatively insensitive to changes in deep chlorophyll maxima, further refinements to the chlorophyll parametrization would not have a significant impact on computed, annual primary production for the N. Atlantic. Given that much greater uncertainty exists in the algorithms for satellite observations of the surface pigment field, and in the  $P-I$  parameters, it is difficult to argue that further improvements in the parametrization of the chlorophyll profile should be accorded high priority.

#### *Effect of the improved P-I data base*

If the basin-scale computations are repeated for the latitudinal regions, with the improved local algorithm and the improved chlorophyll-profile parameters, but with the  $P-I$  parameter set reported by Platt *et al.* (1991) based on a much smaller data set (248 observations, compared to 1862 in the present study), then the annual production obtained is 9.1 Gt C  $y^{-1}$ , instead of 9.9 Gt C  $y^{-1}$ . The differences at the scale of the latitudinal regions are often greater than 20%, and sometimes even greater than 50%. Thus, the computed primary production appears to be more sensitive to changes in the  $P-I$  parameters than in the chlorophyll-profile parameters. At the same time, we have much less data on photosynthesis performance than on chlorophyll profiles. Therefore, more

information on the distributions of  $P-I$  parameters and on factors that control these distributions would help improve large-scale computations of primary production. New techniques for measuring  $P-I$  parameters in natural sea-water samples have just become available (Falkowski and Kolber, 1993; Kolber and Falkowski, 1993). This technique is fast and non-destructive, and if proven to be robust, should go a long way towards filling in the gaps in our knowledge of the distribution of  $P-I$  parameters in nature.

### *Residual problems with satellite algorithms*

Because we are interested in recovering the chlorophyll profile rather than simply a weighted surface chlorophyll, we used a semi-analytical algorithm for retrieving the near-surface chlorophyll field from satellite data (Sathyendranath and Platt, 1989), rather than the NASA algorithm (Gordon and Morel, 1983). Platt *et al.* (1991) showed that the primary production in the N. Atlantic would be reduced by some 50% if the empirical NASA chlorophyll algorithm were used in the computations instead of the Sathyendranath and Platt (1989) algorithm. The differences in computed primary production due to differences in the extrapolation schemes, which have been discussed here at some length, do not generate differences of this magnitude. One may therefore suggest that the greatest uncertainty in basin-scale computations arises not from the extrapolations of *in situ* observations, but from the satellite chlorophyll algorithm. Other recent comparisons of chlorophyll-retrieval algorithms have also shown that considerable differences exist in estimated biomass (Mitchell and Holm-Hansen, 1991; Sullivan *et al.*, 1993; McClain *et al.*, 1994). For this reason alone, if not any other, the exercise presented here should be viewed as a demonstration of how various data sets can be combined to attempt basin-scale computations, rather than as a final answer to the problem. Therefore, the next major step required for refinement of primary production estimates for the N. Atlantic is to improve the chlorophyll algorithm. Given the improved technical capabilities of the next generation of ocean-colour satellites, such as the SeaWiFS, and recent improvements to models of ocean colour (Gordon *et al.*, 1988; Morel and Gentili, 1991; 1993), one hopes that analytical or semi-analytical algorithms for biomass retrieval, with global applicability, would soon come into standard use.

Finally, in our computations, 27% of the total North Atlantic production occurs within the coastal boundary, as we have used the term. The CZCS algorithms are not reliable in coastal regions, because surface chlorophyll is overestimated by the CZCS algorithm in the presence of dissolved organic matter (Sathyendranath and Morel, 1983). Light penetration in coastal waters is also likely to be influenced independently by substances other than phytoplankton, a factor not accounted for in the light transmission model used here. If, for example, the coastal production is over-estimated in our computation by 50% due to the performance of the CZCS algorithm in coastal waters, then our estimate of North Atlantic primary production should be reduced by 13% to  $9.11 \text{ Gt C y}^{-1}$ . Improved biomass algorithms, applicable to coastal waters, are required to address this problem more quantitatively. An additional requirement is the ability to quantify optically-active substances other than phytoplankton to improve our estimates of light transmission. It is expected that the radiometers of satellites such as SeaWiFS will be able to meet these requirements better than the CZCS radiometer carried by the Nimbus satellite (McClain *et al.*, 1992).

## CONCLUSIONS

We have presented a method to partition the North Atlantic, based on knowledge of the near-surface oceanography and of algal response to physical forcing. The motivation for the partition was to facilitate the computation of primary production at large horizontal scales. However, it should also be applicable for other types of calculation in ocean biogeochemistry. In developing the partition, in addition to relying on oceanographic intuition, we used a data base of some 6280 chlorophyll profiles, parametrized for their shape according to a standard equation (shifted Gaussian), and 1862 sets of photosynthesis parameters. The partition divides the ocean into a set of biogeochemical provinces whose nominal boundaries, as well as being plausible to oceanographic insight, are also consistent with the observed patterns, considered seasonally, in this data base.

At the basin scale, calculation of annual primary production is relatively insensitive to the details of the extrapolation protocol. Thus, using our rational partition, we computed an annual production for the North Atlantic basin of  $10.5 \text{ Gt C y}^{-1}$ , compared with a result of  $9.9 \text{ Gt C y}^{-1}$  obtained with a much cruder partition based only on latitude.

At the regional and finer scales, however, the picture is very different, with province-scale discrepancies in excess of 30% between the two calculations, and it is clear that the lack of basin-scale sensitivity is more apparent than real. Certainly, the visual impact of the computed primary production is much more plausible for the rational partition than for the latitudinal one. Moreover, in monitoring the ocean to detect possible responses in it to the suite of processes collectively known as global change, the spatial distribution of primary production will be at least as important a property as its integral over the basin. We therefore support the view that the rational partition is the one to be preferred.

Taking into account the vertical distribution of chlorophyll leads to small, but systematic differences in the calculated primary production (9% at the basin scale, up to 19% at the province scale) compared with an approach that would assume a uniform chlorophyll distribution of magnitude equal to the satellite-retrieved value. Because these errors are systematic, rather than random, the effort involved in correcting for them is certainly justified. However, further refinement of the data base on vertical distribution of chlorophyll is not likely to yield significant improvement in the estimates of primary production at the basin scale.

This is certainly not the case for the photosynthesis parameters: expansion of their data base would definitely be worthwhile, particularly in those provinces and seasons for which, at present, we have no data at all. It could be argued that a more effective approach would be to estimate the photosynthesis parameters from environmental covariates, especially those accessible to remote sensing. However, to construct an estimation procedure one requires a body of data as a starting point. We need to know the initial slope of the light saturation curve as well as the assimilation number. At present, we have neither the data base nor the insight required to construct an estimation procedure for them, and there seems to be no alternative to the challenge of extending their data base.

Finally, we must remark that, although the dearth of data on the photosynthesis parameters is unsatisfactory, imprecision in the retrieval of chlorophyll concentration remains a greater source of uncertainty in the calculation of primary production from remotely-sensed ocean colour.

*Acknowledgements*—This work would not have been possible but for a great number of people whose painstaking measurements of chlorophyll profiles were made available to us. The sources of all the data used are

listed in our Table 1 and we sincerely thank all the people responsible for the data. We also thank those scientists at NASA, especially Gene Feldman and Norman Kuring, who processed and made available the satellite data used in this study. The work presented in this paper was supported by the European Space Agency, with additional support from the Office of Naval Research; the National Aeronautics and Space Administration; the Department of Fisheries and Oceans, Canada; the Natural Sciences and Engineering Research Council; and the Department of National Defence, Canada. This work was carried out as part of the Canadian contribution to the Joint Global Ocean Flux Study. We thank Cathy Porter and George White for their help with the data analysis.

## REFERENCES

- Bishop J. K. B. and W. B. Rossow (1991) Spatial and temporal variability of global surface solar irradiance. *Journal of Geophysical Research*, **96**, 16,839–16,858.
- Brock J., S. Sathyendranath and T. Platt (1993) Modeling the seasonality of subsurface light and primary production in the Arabian Sea. *Marine Ecology Progress Series*, **101**, 209–221.
- Emery W. J., W. G. Lee and L. Magaard (1984) Geographic and seasonal distributions of Brunt-Väisälä frequency and Rossby radii in the North Pacific and North Atlantic. *Journal of Physical Oceanography*, **14**, 294–317.
- Falkowski P. and Z. Kolber (1993) Estimating phytoplankton photosynthesis by active fluorometry. In: *Measurement of primary production from the molecular to the global scale*, W. K. W. Li and S. Y. Maestrini, editors, International Council for the Exploration of the Sea, Copenhagen, pp. 92–103.
- Gordon H. R. and A. Morel (1983) *Remote assessment of ocean color for interpretation of satellite visible imagery. A review*, R. T. Barber, N. K. Mooers, M. J. Bowman and B. Zeitzschel, editors, Springer-Verlag, New York, 114 pp.
- Gordon H. R., O. B. Brown, R. H. Evans, J. W. Brown, R. C. Smith, K. S. Baker and D. K. Clark (1988) A semianalytic radiance model of ocean color. *Journal of Geophysical Research*, **93**, 10,909–10,924.
- Johannessen O. M. (1986) Brief overview of the physical oceanography. In: *The nordic seas*, B. G. Hurdle, editor, Springer-Verlag, New York, pp. 103–127.
- Kolber Z. and P. G. Falkowski (1993) Use of active fluorescence to estimate phytoplankton photosynthesis *in situ*. *Limnology and Oceanography*, **38**, 1646–1665.
- Lighthill M. J. (1969) Dynamic response of the Indian Ocean to the onset of the SW monsoon. *Philosophical Transactions of the Royal Society. London. Series A.*, **265**, 45–93.
- Longhurst A. (1993) Seasonal cooling and blooming in tropical oceans. *Deep-Sea Research*, **40**, 2145–2165.
- Longhurst A. (1995) Seasonal cycles of pelagic production and consumption. *Progress in Oceanography*, (in press).
- Lorenzen C. J. (1970) Surface chlorophyll as an index of the depth, chlorophyll content, and primary productivity of the euphotic layer. *Limnology and Oceanography*, **15**, 479–480.
- McClain C. R., W. E. Esaias, W. Barnes, B. Guenther, D. Endres, S. Hooker, G. Mitchell and R. Barnes (1992) *SeaWiFS calibration and validation plan*. *NASA tech. memo.*, **3**, 1–41.
- McClain C. R., J. C. Comiso, R. S. Fraser, J. K. Firestone, B. D. Schieber, E.-N. Yeh, K. R. Arrigo and C. W. Sullivan (1994) SeaWiFS Technical Report Series, Volume 13, Case studies for SeaWiFS calibration and validation, Part 1. *NASA Technical Memorandum* 104566, **13**, 78 pp.
- Melillo J. M., A. D. McGuire, D. W. Kicklighter, B. Moore III, C. J. Vorosmarty and A. L. Schloss (1993) Global climate change and terrestrial net primary production. *Nature*, **363**, 234–240.
- Miller R. G. (1966) *Simultaneous statistical inference*. McGraw-Hill, NY, pp. 880–891.
- Mitchell B. G. and O. Holm-Hansen (1991) Bio-optical properties of Antarctic Peninsula waters: differentiation from temperate ocean models. *Deep-Sea Research*, **38**, 1009–1028.
- Mittelstaedt E. (1991) The ocean boundary along the northwest African coast: circulation and oceanographic properties at the sea surface. *Progress in Oceanography*, **26**, 307–355.
- Morel A. and J.-F. Berton (1989) Surface pigments, algal biomass profiles, and potential production of the euphotic layer: Relationships reinvestigated in view of remote-sensing applications. *Limnology and Oceanography*, **34**, 1545–1562.
- Morel A. and B. Gentili (1991) Diffuse reflectance of oceanic waters: its dependence on sun angle as influenced by the molecular scattering contribution. *Applied Optics*, **30**, 4427–4438.
- Morel A. and B. Gentili (1993) Diffuse reflectance of oceanic waters. II Bidirectional aspects. *Applied Optics*, **32**, 6864–6879.

- Philander S. G. (1985) Tropical oceanography. *Advances in Geophysics*, **28A**, 461–477.
- Platt T. and A. W. Herman (1983) Remote sensing of phytoplankton in the sea: Surface layer chlorophyll as an estimate of water-column chlorophyll and primary production. *International Journal of Remote Sensing*, **4**, 343–351.
- Platt T. and S. Sathyendranath (1988) Oceanic primary production: Estimation by remote sensing at local and regional scales. *Science*, **241**, 1613–1620.
- Platt T. and S. Sathyendranath (1991) Biological production models as elements of coupled, atmosphere-ocean models for climate research. *Journal of Geophysical Research*, **96**, 2585–2592.
- Platt T. and S. Sathyendranath (1993) Estimators of primary production for interpretation of remotely sensed data on ocean color. *Journal of Geophysical Research*, **98**, 14,561–14,576.
- Platt T., S. Sathyendranath, C. M. Caverhill and M. R. Lewis (1988) Ocean primary production and available light: Further algorithms for remote sensing. *Deep-Sea Research*, **35**, 855–879.
- Platt T., C. Caverhill and S. Sathyendranath (1991) Basin-scale estimates of oceanic primary production by remote sensing: The North Atlantic. *Journal of Geophysical Research*, **96**, 15,147–15,159.
- Platt T., S. Sathyendranath, O. Ulloa, W. G. Harrison, N. Hoepffner and J. Goes (1992) Nutrient control of phytoplankton photosynthesis in the Western North Atlantic. *Nature*, **356**, 229–231.
- Platt T., S. Sathyendranath, I. Joint and M. J. R. Fasham (1993) Photosynthesis characteristics of the phytoplankton in the Celtic Sea during late spring. *Fisheries Oceanography*, **2**, 191–201.
- Prieur L. and S. Sathyendranath (1981) An optical classification of coastal and oceanic waters based on the specific spectral absorption curves of phytoplankton pigments, dissolved organic matter, and other particulate materials. *Limnology and Oceanography*, **26**, 671–689.
- Sathyendranath S. and A. Morel (1983) Light emerging from the sea—interpretation and uses in remote sensing. In: *Remote sensing applications in marine science and technology*, A. P. Cracknell, editor, D. Reidel Publishing Company, Dordrecht, pp. 323–357.
- Sathyendranath S. and T. Platt (1988) The spectral irradiance field at the surface and in the interior of the ocean: A model for applications in oceanography and remote sensing. *Journal of Geophysical Research*, **93**, 9270–9280.
- Sathyendranath S. and T. Platt (1989) Remote sensing of ocean chlorophyll: Consequence of non-uniform pigment profile. *Applied Optics*, **28**, 490–495.
- Sathyendranath S. and T. Platt (1993) Remote sensing of water-column primary production. In: *Measurement of primary production from the molecular to the global scale*, W. K. W. Li and S. Y. Maestrini, editors, ICES Marine Science Symposia, Vol. 197, Copenhagen, pp. 236–243.
- Sathyendranath S., T. Platt, C. M. Caverhill, R. E. Warnock and M. R. Lewis (1989) Remote sensing of oceanic primary production: Computations using a spectral model. *Deep-Sea Research*, **36**, 431–453.
- Sathyendranath S., T. Platt, E. P. W. Horne, W. G. Harrison, O. Ulloa, R. Outerbridge and N. Hoepffner (1991) Estimation of new production in the ocean by compound remote sensing. *Nature*, **353**, 129–133.
- Smith R. C. (1981) Remote sensing and depth distribution of ocean chlorophyll. *Marine Ecology Progress Series*, **5**, 359–361.
- Smith W. O. J. and E. Sakshaug (1990) Polar phytoplankton. In: *Polar oceanography. Part B: chemistry, biology and geology*, W. O. J. Smith, editor, Academic Press, New York, pp. 477–525.
- Sullivan C. W., K. R. Arrigo, C. R. McClain, J. C. Comiso and J. Firestone (1993) Distributions of phytoplankton blooms in the Southern Ocean. *Science*, **262**, 1832–1837.
- Sverdrup H. U. (1953) On conditions for the vernal blooming of phytoplankton. *Journal du Conseil*, **18**, 287–295.
- Toggweiler J. R. (1990) Modelling workshop offers first look at new simulation of Equatorial Pacific. *US JGOFS News*, **2**, 1, 11.
- Topliss B. J. and T. Platt (1986) Passive fluorescence and photosynthesis in the ocean: implications for remote sensing. *Deep-Sea Research*, **33**, 849–864.
- Tomczak M. and J. S. Godfrey (1994) *Regional oceanography: an introduction*. Pergamon, New York, 422 pp.
- Venrick E. L. (1988) The vertical distributions of chlorophyll and phytoplankton species in the North Pacific central environment. *Journal of Plankton Research*, **10**, 987–998.
- Yentsch C. S. (1965) Distribution of chlorophyll and phaeophytin in the open ocean. *Deep-Sea Research*, **12**, 653–666.